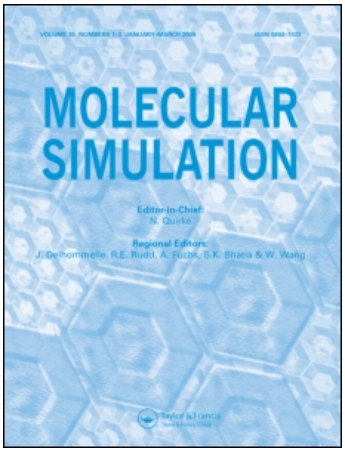

Molecular Simulation
Publication details, including instructions for authors and subscription information:
http://www.informaworld.com/smpp/title~content=t713644482

Study on the hydrolysis mechanism of phosphodiesterase 4 using molecular dynamics simulations

N. S. Kang[a]; C. H. Chae[a]; S. -E. Yoo[a]
[a] Korea Research Institute of Chemical Technology, Taejeon, South Korea

To cite this Article Kang, N. S. , Chae, C. H. and Yoo, S. -E.(2006) 'Study on the hydrolysis mechanism of phosphodiesterase 4 using molecular dynamics simulations', Molecular Simulation, 32: 5, 369 — 374
To link to this Article: DOI: 10.1080/08927020600717111
URL: http://dx.doi.org/10.1080/08927020600717111

Molecular Simulation, Vol. 32, No. 5, 30 April 2006, 369–374

Taylor & Francis
Taylor & Francis Group

Study on the hydrolysis mechanism of phosphodiesterase 4 using molecular dynamics simulations

N. S. KANG*, C. H. CHAE and S.-E. YOO

Korea Research Institute of Chemical Technology, PO Box 107, Yusung-gu, Taejeon 305 343, South Korea

(Received January 2006; in final form March 2006)

We carried out NPT molecular dynamics simulations in an explicit solvent to better understand the mechanism of cyclic adenosine monophosphates (cAMP) hydrolysis by phosphodiesterase 4 (PDE4) enzyme on atomic details and to obtain information on the dynamics characteristic of the catalytic domains of PDE4. In analyzing the water hydrogen-bond network around the active site, we also showed the importance of water in drug–protein interactions. In addition, we reported the characteristics of the hydration pattern and the dynamic distance distribution around the interesting residues. The results indicated that Asp318 plays the role of a general base that can activate water molecule for nucleophilic attack on cAMP. As expected, His160 plays the role of a proton donor for cAMP.

Keywords: PDE4; cAMP; Molecular dynamics simulation; Hydrolysis mechanism; Hydration pattern

1. Introduction

Cyclic nucleotide phosphodiesterases (PDEs) [1–4] are enzymes that comprise 11 families. They hydrolyze cyclic 3′, 5′-adenosine and guanosine monophosphates (cAMP and cGMP), which are intracellular second messengers, to AMP and GMP and this type of hydrolysis is the only way to inactivate cAMP. PDEs are therefore importance for regulating of cyclic nucleotide concentration in the cell. All PDE families share a conserved catalytic domain of about 330 amino acids in the carboxy terminal half of the protein (18∼46% of sequence identity). Each PDE family has different substrate preferences and selective inhibitors [5–7].

There are three types of PDEs; cAMP-specific (PDE4ABCD, PDE7AB and PDE8AB), cGMP-specific (PDE5A, PDE6ABC and PDE9A) and dual-specific (PDE1ABC, PDE2A, PDE3AB, PDE10A and PDE11A) [8–9]. The cAMP-specific type 4 PDE (PDE4) is the enzyme that is related to the metabolism of cAMP in immune and inflammatory cells such as eosinophils, T lymphocytes, macrophages, neutrophils, dentritic and epithelial cells. Recently, PDE4 inhibitors have been developed as new therapeutic agents for inflammatory diseases such as asthma and chronic obstructive pulmonary disease (COPD) [10–13].

Many available crystal structures of the PDE families and their inhibitor-bound complex structures have been deposited at the protein data bank [14–21]. It is to notice that Huai *et al.,* reported the crystal structure of PDE4 in a complex with AMP, the product of catalysis [14]. They suggested two tentative mechanisms for the hydrolysis of the cAMP phosphodiester bond; and in these mechanisms, a hydroxide ion or a water molecule bridges two metal ions. They also suggested that Asp318 or Glu230 residues in PDE4 catalytic domains might serve as a general base for activating a water molecule, which attacks the phosphorus atom. In addition, they said that His160 serves as a general acid that donates a proton to the O3′ atom of cAMP. The study on the product-bound enzyme could give an indirect information on the catalytic mechanism, but fails to adequately explain the catalytic mechanism of cyclic nucleotide hydrolysis by PDE on atomic details.

In our study, we therefore aimed at better understanding the mechanism of the enzyme reaction and gaining insight into the design of PDE4 selective inhibitors. To this end, we report on the preferential mechanism of the hydrolysis of cAMP reactant by PDE4 with atomic details. We also report on the dynamic characteristics of the catalytic domains of PDE4, which was examined by using NPT molecular dynamics simulations in an explicit solvent environment.

*Corresponding author. Tel: +82-42-860-7452. Fax: +82-42-860-7635. Email: nskang@krict.re.kr

Molecular Simulation
ISSN 0892-7022 print/ISSN 1029-0435 online © 2006 Taylor & Francis
http://www.tandf.co.uk/journals
DOI: 10.1080/08927020600717111

2. Methods

We carried out two molecular protein dynamics simulations in an explicit solvent environment; in one simulation, we used a water solution including only PDE enzyme molecule (free PDE) as a comparison; in the other, we used a cAMP-bound PDE complex in a water solution. For each simulation, which involved 1.01 ns with a step size 1.0 fs, we used CHARMM force field parameters (version 29.0) [22] and the TIP3P [23] water model. The initial structure of the cAMP-bound PDE complex was taken from the protein data bank entry 1PTW, which represents the AMP-bound PDE4D. To optimize the conformation and atomic charges of the cAMP, we used a quantum calculation using HF/6-31G basis set of GAUSSIAN98. We then adjusted the assigned charges of cAMP to the CHARMM force field to preserve the consistency with the protein force field. The free PDE and cAMP–PDE complex were solvated in a water box of dimension $71.3\times62.0\times62.0$ Å and periodic boundary condition was applied during all simulations. There were 7441 and 7428 TIP3P water molecules for PDE and cAMP–PDE complex, respectively. The metals were zinc ions and we tried at various charge values ($+0.5$, $+0.75$, $+1.5$ and $+2.0$) for zinc ion to generate a correct conformation around zinc ion of PDE molecule. Finally, we chosen zinc ion charge as $+0.75$.

Before conducting the molecular dynamics simulations, we relaxed the strained initial structure of the two prepared solvated systems using energy minimization. We then used a twin-range cutoff of 1.2/1.5 nm, firstly, for the heating process during 10 ps from 0 to 298 K, secondly, for the following equilibration of 700 ps and finally, for the 300 ps production simulations for statistical analysis. After the heating process, all simulations were performed in the NPT ensemble with a leapfrog integration algorithm considered to be the most stable in NPT molecular dynamics. To control the temperature and pressure of the systems, we used the Langevin piston method [24] with 225 amu for the mass of the pressure and 1000 kcal ps^2 for the mass of the thermal piston under 1 atm. For the collision frequency, we chose 25 ps^{-1}. A switching function for the van der Waals interaction and a shifting function for the electrostatic interaction were used to smoothly reduce the energies and to avoid discontinuities in the energies. Finally, for the initial structural setup and visualization, we used an in-house molecular modeling package called WinPro.

3. Results and discussion

To ensure that the two simulations reached equilibrium after 700 ps, we calculated the RMS fluctuations of the C_α atoms converged to an average value of less than 1.0 Å for each simulation. The conformations of metal binding sites were similar to those of a crystal structure; moreover, the metal atoms were coordinated with the same residues in the crystal structure. Having confirmed the overall stability of the two protein molecular dynamics simulations, we collected coordinate sets at 1 ps interval during next 300 ps of the production simulation. We then analyzed the following factors: the interaction between cAMP and PDE4D residues, the characteristics of water molecules within the first hydration shell of the comparison simulation and also the dynamic distance fluctuation between important residues of PDE4D and cAMP atoms

3.1. Characteristics of the hydrogen-bond network and the dynamics within the active site atoms

Table 1 compares the calculated results for the hydrogen-bond distances between cAMP and the active site residues of PDE4D with the results of the AMP-bound PDE4D X-ray crystal structure. As reported in before-mentioned crystal structure [14], the adenine group of the cAMP forms three hydrogen bonds with Gln369 and Asn321 residues. The phosphate group of cAMP is positioned near the His160 residue as well as two metal sites. In free PDE4D simulation, the side chain atoms of Gln369 fluctuate and thus its hydrogen bond with Tyr329 is reversed as shown in figure 1. When analyzing the crystal structure of PDE families to explain the cAMP- or cGMP-selectivity, Zhang *et al.,* based their assumptions on the glutamine switching mechanism [7]. During the dynamics process of our simulation, however, we can reverse the orientation of the side chain atoms of Gln369 depending on changes in the interactions with the adjacent residue, Tyr329. On the other hand, in the cAMP-bound PDE4D complex simulation, the side chain atoms of Gln369 are well constrained and they preserve the hydrogen bond with the adenine group of cAMP. Further study is needed on the dynamic properties of Gln369 residues in other PDE families.

To investigate the effect of water molecules, we analyzed the hydrogen-bonded circular network, ring structure, of the water molecules within 25 Å from the center of mass of the Gln369 as shown in table 2. We also analyzed the interaction energies between the surrounding water molecules. To analyze the ring structure of the water, we used the energetic criterion of -2.25 kcal/mol or less, which corresponds to the minimum of the pair energy distribution of the TIP3P water potential. Detailed

Table 1. The hydrogen bond distances between atoms of cAMP with the active site residues of PDE4D.

cAMP atom	*PDE4D atom*	*Distance in crystal structure (Å)*	*Distance in our simulation (Å)*
N1	Gln369 NE2	3.09	3.07
N6	Asn321 OD1	2.84	3.05
N7	Asn321 ND1	3.19	3.12
O2P	His160 NE2	2.89	2.96
O3′	His160 NE2	4.00	3.59

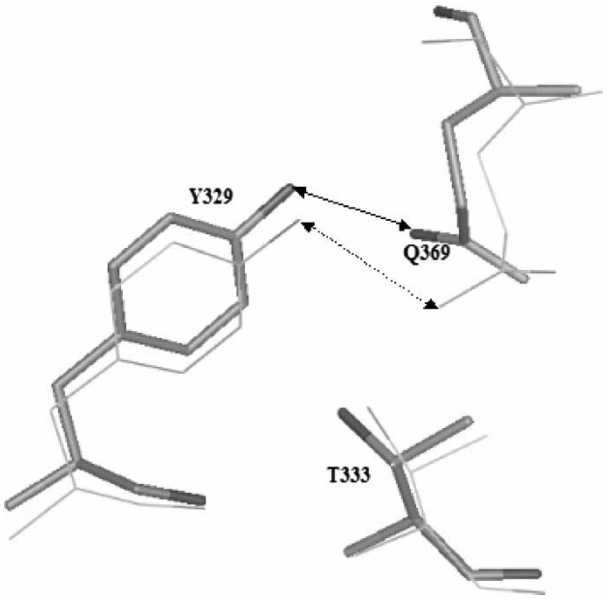

Figure 1. Orientation of the side chain atoms of Glu369. The sticks representation is the final structure of the free PDE4D simulation and the line conformation shows the initial structure based on the 1PTW entry.

explanations for selecting the ring structure are given in a previous work of Kang *et al.* [25]. The ring structure in the free PDE4D simulation was quite different from that of the cAMP-bound PDE4 complex simulation. The energy of the ring cluster energy and the total energy of the water–water interaction were also smaller in the cAMP-bound PDE4 complex system than in the free PDE4 system. These results show that the water ordering is important for substrate–protein interaction.

3.2. The hydration characteristics around the Glu230 and Asp318 residues in free PDE4D simulation

To investigate the solvent effect around Glu230 and Asp318 residues, we counted the water molecules within 5.0 Å from each of the two residues and we calculated the surface area of the two residues during the free PDE4D simulation. The orientational information of the hydration shell around the two residues was obtained by using the dipole direction of the hydrated water molecules. Table 3 shows the averaged results for the water molecules within 5 Å of the hydration shell around the two residues. In figure 2, we also report the number of water molecules and the distribution of $N_{\theta>90°}/N_{\theta<90°}$ in the process of the final 300 ps production simulation. The ratio $N_{\theta>90°}/N_{\theta<90°}$, the number of water molecules with $\theta>90°$ to that with $\theta<90°$, means the extent to which the water molecules in the hydration shell are orientated in such a way that the water O–H bond radiates out of the residues [26]. The z-axis of water molecule is the vector opposite to the electric dipole moment of water molecule.

Table 2. Information about the water molecules in the hydration shell within 25 Å from the Gln369.

	PDE4D	*PDE4D+cAMP*
3-ring	45.16(15.72%)	78.52(16.81%)
4-ring	61.20(21.30%)	121.05(25.91%)
5-ring	85.03(29.60%)	87.59(18.75%)
6-ring	95.94(33.39%)	180.03(38.53%)
3-ring cluster energy*	−11.77	−13.20
4-ring cluster energy	−17.05	−20.59
5-ring cluster energy	−23.15	−26.95
6-ring cluster energy	−28.53	−33.80
W–W interaction energy*	−6513.62	−8109.6
Average number of water	934.69	925.35

*The used energy unit is kcal/mol.

Table 3. The characteristics of water molecules in a 5 Å hydration shell of Glu230 and Asp318 residues for free PDE4D simulation.

Residues	SASA* (Å^2)	*Number of water molecules*	$N_{\theta>90°}/N_{\theta<90°}$
Glu230	439.63	7.92	0.20
Asp318	415.36	10.15	0.08

*SASA means solvent accessible surface area.

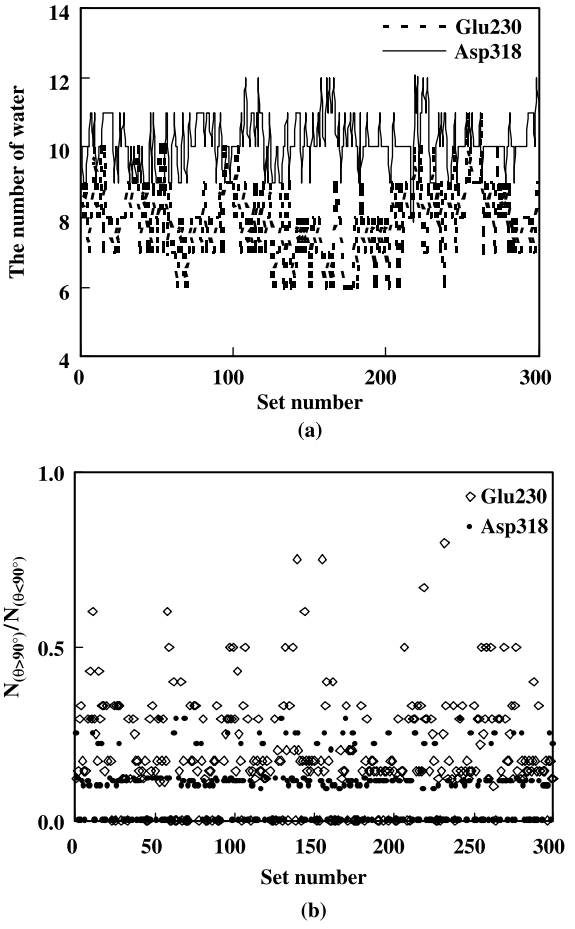

Figure 2. (a) Number of water molecules and (b) distribution of $N_{\theta>90°}/N_{\theta<90°}$ within the 5 Å hydration shell around Glu230 and Asp318 during the final 300 ps production simulation.

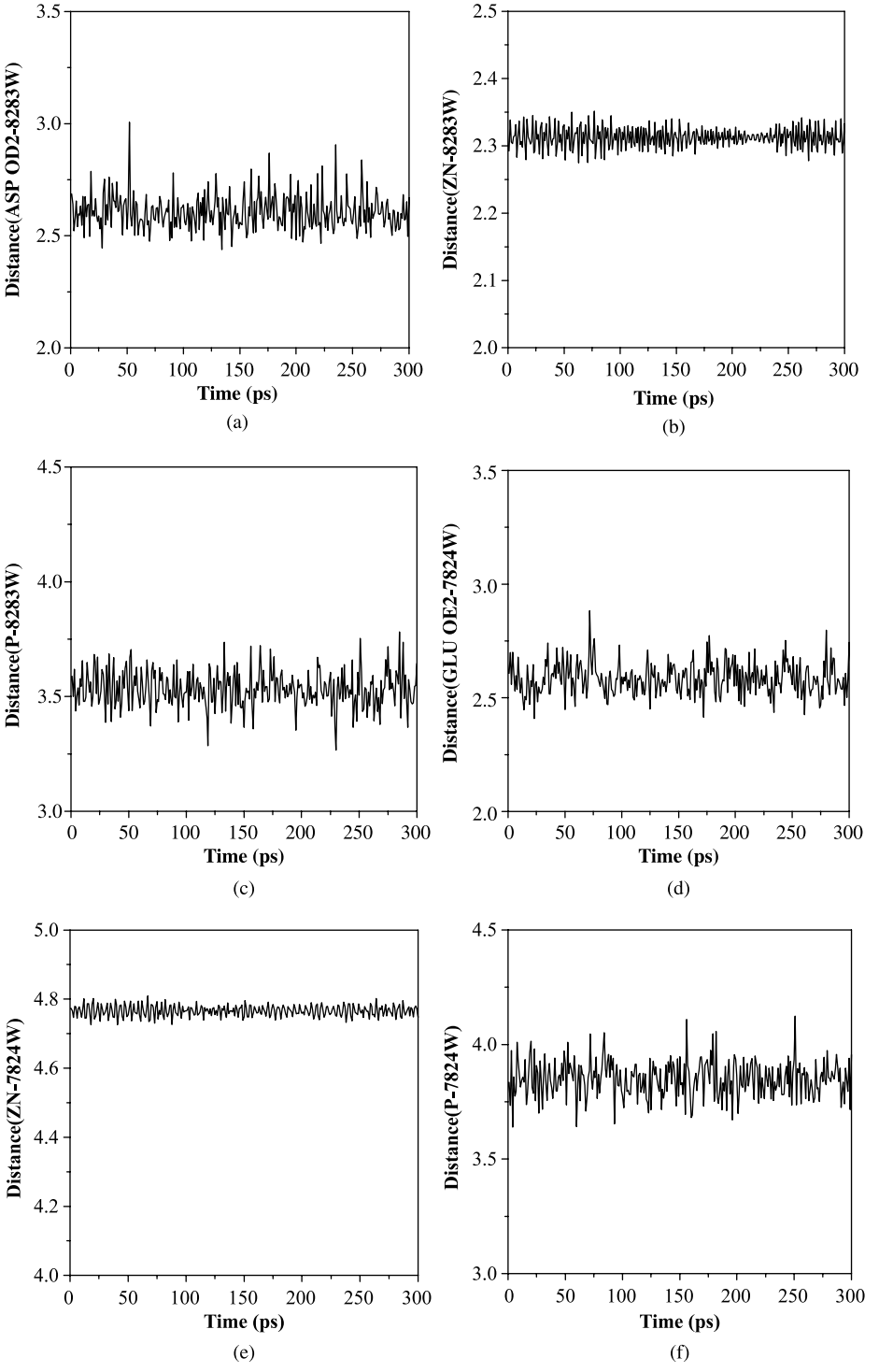

Figure 3. Dynamic distance between the Asp318 and 8283th water molecule, between Glu230 and 7824th water molecule, between the metal ion and each residue and phosphorus atom and each water molecule. (a) Asp318 residue OD2 atom and 8283th water molecule; (b) zinc atom and 8283th water molecule; (c) phosphorus atom and 8283th water molecule; (d) Glu230 residue OE2 atom and 7824th water molecule; (e) zinc atom and 7824th water molecule; and (f) phosphorus atom and 7824th water molecule.

$$\cos\theta = \mu_{\mathrm{co}} \cdot \mu_z, \quad \mu_{\mathrm{co}} = \frac{(r_{\mathrm{cc}} - r_o)}{|r_{\mathrm{cc}} - r_o|};$$

where μ_z is the unit vector in z direction and r_{cc} is the vector to the center of mass of each corresponding residue.

Given that Glu230 and Asp318 are both hydrophilic, about half or more of the water molecules must point inwards. However, Asp318 attracts more the water molecules causing a stronger interaction with water, because $N_{\theta>90^\circ}/N_{\theta<90^\circ}$ value is less for Asp318 than for Glu230. On Basis of these results, we expect Asp318 residue to act as a general base for activate water molecules for a nucleophilic attack on the phosphorus atom of cAMP.

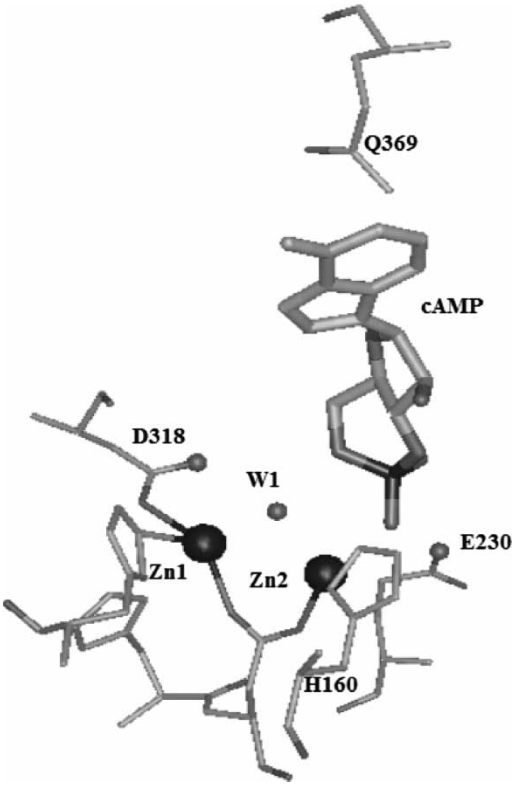

Figure 4. The conformation for the hydrolysis mechanism of the cAMP by PDE4.

3.3. The dynamic distance distributions between important atoms for a hydrolysis mechanism

To confirm our facts, we investigated the dynamic distance distribution for the different pair of atoms. Figure 3(a)–(f) shows the results. In each simulation, an OD2 atom of Asp318 interacts with an 8283th water molecule (W1) at around ∼2.5 Å during 300 ps simulation (figure 3(a)). The W1 molecule simultaneously interacts with a zinc metal atom (figure 3(b)), offering the proper direction for attacking the phosphorus atom of cAMP. Furthermore, as shown in figure 3(c), an O atom of the W1 water molecule that interacts with Asp318 is positioned at around 3.5 Å from the phosphorus atom of cAMP. A W1 molecule can therefore be activated as a nucleophile by Asp318 and by a zinc atom. Figure 4 shows the W1 molecule's position, which is bi-coordinated by the OD2 atom 318D and the zinc metal ion. On the other hand, an OE2 atom of Glu230 also interacts with a 7284th water molecule at a distance of 2.5 Å (figure 3(d)), which is similar to that of Asp318, though the water molecule does not interact with the adjacent zinc atom (figure 3(e)). This phenomenon shows that a water molecule that interacts with Glu230 is an inappropriate molecule for attacking the phosphorus atom of cAMP. In addition, as shown in figure 3(f), an O atom of the water molecule that interacts with Glu230 is positioned around 4.0 Å from the phosphorus atom of the cAMP and this distance is farther than that of Asp318. From the results of the distance distribution, we are convinced that Asp318 residue is better general base

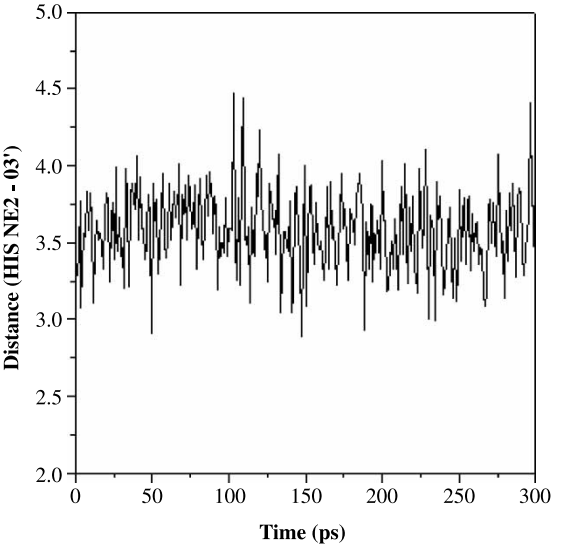

Figure 5. The dynamic distance between the O3′ atom of the general base His160 residue NE2 atom and P atom of cAMP.

for converting cAMP to AMP than Glu230 residue. In figure 5, we reported the dynamic distance fluctuation between the NE2 atom of His160 residue and the O3′ atom of cAMP's phosphate group. During 300 ps final simulation, His160 residue NE2 is approximately 3.5 Å from the cAMP's O3′ atom. This fact confirms the important potential role of His160 residue as a proton donor to the O3′ atom to complete the hydrolysis of the cAMP. Moreover, studies showing that the mutation of the His160 residue reduces the catalytic activity of PDE4 confirm the importance of the His160 residue as a proton donator [27].

4. Conclusion

By using NPT molecular dynamics simulations, we studied how the PDE4 enzyme's hydrolysis of cAMP affects the atomic details. To clearly show the importance of water molecules in drug–protein interactions, we analyzed the water hydrogen-bond network or ring structure around the active site of the Gln369 residue. The water hydrogen-bond network is an important feature of the de novo design of PDE inhibitors. To clearly show the preferential mechanism, we also investigated the characteristics of the hydration pattern and the dynamic distance distribution around particular residues. The W1 molecule, which is coordinated by the OD2 atom of Asp318 as general base and by zinc metal ions, acts as a nucleophile that attacks the phosphorous atom of cAMP. Our study also supports the well-known view that His160 donates a proton to the O3′ atom to complete the hydrolysis of cAMP to AMP. The two metal sites have been considered an important site for interactions between PDE4 and its inhibitors. The results of this study offer insights into the design of new PDE4 inhibitors that can facilitate interaction around the two metal sites.

Acknowledgement

This research was supported by a grant (CBM2-B511-001-1-0-0) from the Center for Biological Modulators of the 21st Century Frontier R & D Program, the Ministry of Science and Technology, Korea.

References

[1] J.A. Beavo. Cyclic nucleotide. phosphodiesterases; functional implications of multiple isoforms. *Physiol. Rev.*, **75**, 725 (1995).
[2] M. Conti. Phosphodiesterases and cyclic nucleotide. signaling in endocrine cells. *Mol. Endocrinol.*, **14**, 1317 (2002).
[3] M. Conti, S.L. Jon. The molecular biology of cyclic nucleotide. phosphodiesterases. *Prog. Nucleic Acid Res. Mol. Biol.*, **63**, 1 (1999).
[4] S.H. Soderling, J.A. Beavo. Regulation of cAMP and cGMP signaling; new phosphodiesterases and new functions. *Curr. Opin. Cell. Biol.*, **12**, 174 (2000).
[5] S.H. Francis, I.V. Turko, J.D. Corbin. Cyclic nucleotide. phosphodiesterases: relating structure and function. *Prog. Nucleic Acid Res. Mol. Biol.*, **65**, 1 (2001).
[6] L.C. Graeme, P.E. Bruce, Y. Suzuki, D. Fong, B. Powell, B.H. Lee, C. Luu, M. Tabrizizad, S. Gillette, P.N. Ibrahim, D.R. Artis, G. Bollag, M.V. Milburn, S.H. Kim, J. Schiessinger, K.Y.J. Zhang. Structural basis for the activity of drugs that inhibit phosphodiesterases. *Structure*, **12**, 2233 (2004).
[7] K.Y.J. Zhang, G.L. Card, Y. Suzuki, D.R. Artis, D. Fong, S. Gillette, D. Hsieh, J. Neiman, B.L. West, C. Zhang, M.V. Milburn, S.H. Kim, J. Schlessinger, G. Bollag. A glutamine switch mechanism: short article for nucleotide. selectivity by phosphodiesterases. *Mol. Cells*, **15**, 279 (2004).
[8] J.A. Beavo, L.L. Brunton. Cyclic nucleotide. research still expanding after half a century. *Nat. Rev. Mol. Cell Biol.*, **3**, 710 (2002).
[9] C. Mehats, C.B. Anderson, M. Filopani, S.L. Jin, M. Conti. Cyclic nucleotide. phosphodiesterases and their role in endocrine cell signaling. *Trends Endocrinol. Metab.*, **13**, 29 (2002).
[10] T.J. Torphy, G.P. Livi, S.B. Christensen. Novel phosphodiesterase inhibitors for the therapy of asthma. *Drug News Perspect.*, **6**, 537 (1993).
[11] M.N. Palfreyman. Phosphodiesterase inhibitors as antiasthmatic agents. In Annual Reports in Medicinal Chemistry, Vol.29, p.185, Academic Press, New York (1994).
[12] P. Norman. PDE4 inhibitors 1998. *Expert Opin. Ther. Pat.*, **8**, 771 (1998).
[13] M.M. Teixeira, R.W. Gristwood, N. Cooper, P.G. Hallewell. Phosphodiesterase (PDE) 4 inhibitors: anti-inflammatory drugs of the future? *TIPS*, **18**, 164 (1997).
[14] Q. Huai, J. Colicelli, H. Ke. The crystal structure of AMP-bound PDE4 suggests a mechanism for phosphodiesterases catalysts. *Biochemistry*, **42**, 13220 (2003).
[15] Q. Huai, Y. Liu, S.H. Francis, J.D. Corbin, H. Ke. Crystal structure of phosphodiesterases 4 and 5 in complex with inhibitor IBMX suggest a conformation determinant of inhibitor selectivity. *J. Biol. Chem.*, **279**, 13095 (2003).
[16] Q. Huai, H. Wang, Y. Sun, H.Y. Kim, Y. Liu, H. Ke. Three-dimensional structures of PDE4D in complex with roliprams and implication on inhibitor selectivity. *Structure (Camb)*, **11**, 865 (2003).
[17] Q. Huai, H. Wang, W. Zhang, R.W. Colman, H. Robinson, H. Ke. Crystal structure of phosphodiesterase 9 shows orientation variation of inhibitor 3-isobutyl-1-methylxanthine binding. *Proc. Natl. Acad. Sci. USA*, **101**, 9624 (2004).
[18] M.E. Lee, J. Markowitz, J.O. Lee, H. Lee. Crystal structure of phosphodiesterase 4D and inhibitor complex. *FEBS Lett.*, **530**, 53 (2002).
[19] G. Scapin, S.B. Patel, C. Chung, J.P. Varnerin, S.D. Edmondson, A. Mastracchio, E.R. Parmee, S.B. Singh, J.W. Becker, L.H. Van Der Ploeg. Crystal structure of human phosphodiesterase 3B: atomic basis for substrate and inhibitor specificity. *Biochemistry*, **43**, 6091 (2004).
[20] B.J. Sung, K. Yeon Hwang, Y. Ho Jeon, J.I. Lee, Y.S. Heo, J. Hwan Kim, J. Moon, J. Min Yoon, Y.L. Hyun, E. Kim, J.E. Sung, S.Y. Park, J.O. Lee, T.G. Lee, S.G. Ro, J.M. Choe. Structure of the catalytic domain of human phosphodiesterases 5 with bound drug molecules. *Nature*, **425**, 98 (2003).
[21] R.X. Xu, W.J. Rocque, M.H. Lambert, D.E. Vanderwall, M.A. Luther, R.T. Nolte. Crystal structure of the catalytic domain of phosphodiesterase 4B complexed with amp 8-br-AMP, and rolipram. *J. Mol. Biol.*, **337**, 355 (2004).
[22] B.R. Brooks, R.E. Bruccoleri, B.D. Olafson, D.J. States, S. Swaminathan, M. Karplus. CHARMM: a program for macromolecular energy, minimization, and dynamics calculations. *J. Comp. Chem.*, **4**, 187 (1983).
[23] W. Jorgensen, J. Chandrasekhar, J. Madura, R. Imprey, M. Klein. Comparison of simple potential functions for simulating liquid waters. *J. Chem. Phys.*, **79**, 926 (1983).
[24] S.E. Feller, Y. Zhang, R.W. Pastor. Constant pressure molecular dynamics simulation: the Langevin piston method. *J. Chem. Phys.*, **103**, 4613 (1995).
[25] N.S. Kang, D.H. Jung, K.T. No, M.S. Jhon. Molecular dynamics simulation of Na^+-DMP^- and Na^+-MP^{2-} ion pair in aqueous solution. *Chem. Phys. Lett.*, **364**, 580 (2002).
[26] D.H. Jung, N.S. Kang, M.S. Jhon. Site-directed mutation study on hyper thermostability of rubredoxin from pyrococcus furiosus using molecular dynamics simulations in solution. *J. Phys. Chem.*, **101**, 466 (1997).
[27] S. Jacobitz, M.D. Ryan, M.M. McLaughlin, G.P. Livi, W.E. Dewolf, T.J. Torphy. Role of conserved histidines in catalytic activity and inhibitor binding of human recombinant phosphodiesterase 4A. *Mol. Pharmacol.*, **51**, 999 (1997).